BNL-104759-2014-TECH

AGS/AD/Tech Note No. 343;BNL-104759-2014-IR

MAGNETOSTATIC ANALYSIS OF THE AGS H-10 SEPTUM MAGNET

M. A. Goldman

August 1990

Collider Accelerator Department

Brookhaven National Laboratory

U.S. Department of Energy

USDOE Office of Science (SC)

DISCLAIMER

Accelerator Division
Alternating Gradient Synchrotron Department
BROOKHAVEN NATIONAL LABORATORY
Associated Universities, Inc.
Upton, New York 11973

Accelerator Division
Technical Note

AGS/AD/Tech. Note No. 343

MAGNETOSTATIC ANALYSIS OF THE AGS H-10 SEPTUM MAGNET

August 24, 1990

M.A. Goldman

1. Introduction.

The H-10 Septum Magnet is a pulsed, single-turn magnet used for fast beam extraction of the AGS proton beam, downstream from the H-10 superperiod. The magnet is positioned just outside the AGS vacuum beam pipe. A secondary vacuum pipe, of rectangular profile, carrying the extracted beam, lies within the magnet's aperture.

A 2-dimensional magnetostatic computational study of this magnet was carried out using the POISSON family of codes [1,2]. The goal of the study was to examine the following questions:

(1) Should one use a magnetically soft high-permeability steel pipe section locally, as the main ring beam pipe, to shield the circulating AGS beam from the fringing field of the septum magnet? In particular: what are the geometric shape and magnitude of the septum magnet's fringing field; will the shield pipe saturate magnetically; is a high-permeability beam tube better than a non-magnetic beam tube?

(2) How do the height and position of the magnet's septum, and the spacing between septum and flat milled surface on the beam pipe influence the extension of the fringe magnetic field into the main ring beam tube, and the uniformity of the magnetic field in the exit beam tube?

(3) Is the proposed septum magnet design adequate with res-pect to field uniformity in the exit beam tube, and does it give sufficiently low fringing field inside the AGS main beam pipe to allow normal beam operation?

(4) How do measurements of the septum magnet's magnetic field and fringing field outside of the septum [3] compare with the computed values? That is, can we have confidence that a reasonable working knowledge of the magnetic properties of the septum magnet has been achieved?

2. The H-10 Septum Magnet.

Design and construction information for this magnet are to be found in the AGS drawing file: H-10 Ejector Magnet Module (Mark V), Job Number D11-2M-286. Component part design details are found in the drawings: D11-M-11695-Rev C , laminations; D11-M-11727-5, septum; D11-M-11697-5-Rev C, module assembly; D11-M-11741-4, H-10 parameters.

Pulse rise and fall times are 0.5 microseconds, to give a 10 kilogauss magnetic field at 20 kiloampere current.

The aperture is 1 inch, vertical, by 2.7 inches, horizontal. The effective magnet length is 84 inches. The copper septum conductor is tapered linearly from 0.041" up to 0.250" along its length, with mean thickness 0.146"; the return conductor is tapered from 0.341" to 0.544", with mean width 0.443". The conductors are wrapped with one or more turns of 0.0025" thick kapton tape, to insulate them from the magnet laminations and beam pipes. The laminations are formed from sheets of fully processed 24 gage USS type M36 steel.

The main beam pipe profile, near the septum magnet, is that of a circular tube, 6.125" inner diameter and 6.615" outer diameter, with a flat surface milled on the tube at 3.102" distance from the tube's axis. The pipe is made of Lukens Corp. type C-1020 steel.

3. Some Comments On The POISSON Calculations.

In the present study, no attempt was made to perform a dynamical 3-dimensional analysis. Suitable computer codes were not readily available, and a full analysis is of greater order of complexity than the 2-dimensional static study. Even the static study presents difficulties, because large field gradients exist and spatial structures vary rapidly at locations of interest. That is: narrow gaps, re-entrant geometry, discontinuities in 2 permeability and current density and magnetic field direction, as well as rapidly varying permeability all occur in the critical and physically interesting region where the current-carrying copper septum, steel magnet body, and soft steel AGS beam tube meet. (This region is critical because the circulating beam in the AGS ring lies near the beam tube's inner surface, in the fringing field of the septum magnet, at extraction). Also, this region makes up only a small part of the magnetic geometry.

Despite the fact that only a static analysis was performed information relating to:

magnetic saturation of the beam pipe, effects of gap space between septum and beam pipe, septum-to-lamination spacings, internal magnetic field uniformity, as well as leakage field at the peak of the magnetic field pulse, can be obtained from such modelling calculations.

Even in the 2-dimensional magnetostatic model, the complicated and magnetically nonuniform geometry presents problems in setting up the computations. The POISSON codes [1,2] solve the 2-dimensional Poisson equation by means of an over-relaxation procedure on a triangulated partition of the magnet's cross-sectional plane. High resolution in the triangular mesh is needed in the topologically complicated areas where septum, magnet and pipe all meet. The requirement for high resolution, constrained by the limited number of mesh lattice points available in the existing codes, poses computational challenges, particularly with respect to the process of mesh generation.

The mesh is usually generated by running in sequence the codes AUTOMESH and LATTICE. Subsequently the output data from LATTICE is plotted graphically, to display the generated mesh. (This is accomplished by running the LATTICE output on the graphics code TEKPLOT). If the generated triangular mesh is satisfactory, the output from LATTICE is used, together with permeability tables, as the input data for the POISSON code, which actually calculates the magnetic fields. The output data from POISSON is entered into TEKPLOT, which supplies printed magnetic field plots.

The code AUTOMESH has not yet been developed to the stage that it can uniquely recognise and flag distinct topological computational regions with respect to their topological character. In AUTOMESH, a computational region is defined by listing coordinates of successive vertices on a boundary path of the region, and listing the parameters defining a simple arc (either a line or circle or hyperbola) joining them. The AUTOMESH code generates a data output file, TAPE73.DAT, which lists, for each region: the region number, current, material 3 designation integer, logical K and L lattice integer coordinates, and X and Y position coordinates for the boundary path lattice points defining that region. The file TAPE73.DAT provides all of the input data used by the LATTICE code, which generates the logical and position coordinate information for the full set of lattice vertices. But TAPE73.DAT contains insufficient information to define the connectivity of the different computational regions. When the LATTICE code is run, it may generate triangles which overlap one another (negative area triangles) or connect disjoint computational regions by assigning the same logical coordinates to distinct boundary points of different regions.

In Appendix III of this note we describe how to edit the TAPE73.DAT data file to amend this file so that it can run on LATTICE and not generate negative area triangles.

4. <u>Computational Results.</u>

The septum magnet geometry is shown in Figures 1 and 2. A portion of the computational lattice is shown in Figure 3. The magnetic field is symmetric about the horizontal midplane of the magnet, so only the upper half of the magnet is shown. Fields are calculated for this half-magnet geometry, with the boundary condition that the B-field is normal to the midplane. The current carried by each upper half-conductor, in the computation, is half of the magnet current.

The plotted magnetic equipotential lines show the magnetic field's shape near the septum when no shield pipe is used, (Fig. 4) and when the steel shield pipe is present (Fig's 5, 6). In the shield pipe, the leakage flux splits between two low reluctance paths. One path is the flat pipe section near the septum; the other path is the remainder of the pipe wall. Only a small part of the leakage flux penetrates into the interior of the shield pipe. (Each of the field plots displays a limited range of magnetic potential, in order to emphasize the details of the field in different regions of the magnet).

A typical plot of the magnetic equipotential lines in the main magnet aperture is shown in Figure 7.

Calculations were performed for two different configurations of the milled flat surface of the pipe. In the first configuration, a single flat was milled on the (originally cylindrical) pipe surface; in the second configuration, a raised plateau 0.005" high and 1.00" wide was left in the center of the flat (Fig.2) in order to allow the shield pipe to approach the septum more closely. The original magnet design used the second configuration, but the first configuration was used for the actual magnet, as built. The calculation indicated little difference in the fields, for the two configurations.

Magnetic field calculations were made, with no shield pipe present, for configurations which included the following details of the magnet lamination: assembly-bolt penetration holes, alignment notches in the lamination, and the gap space between the current return conductor and the inner vertical lamination edge. The calculations were repeated, omitting the details. The results of the calculations with and without the details were close to each other in the important areas of the magnet main midplane field, and in the leakage field near the septum. These features were omitted from the calculation when when pipe-shielding effects were computed.

The variation of the B-field within the magnet aperture is shown in Figures 8 and 9. Near the conductors the field amplitude increases by an amount which depends on the conductor height within the magnet aperture. The "ears" can can be decreased in size by decreasing the gap (G) between the ends of the septum and the magnet laminations. This behavior has been analyzed by Keizer [7]. When the gap is decreased, the leakage flux near the septum is also decreased.

The variation of the leakage (vertical) B-field at the horizontal magnet midplane, versus distance from the lamination edge of the magnet, is shown in Figures 10 and 11. It is clear that the leakage field is significantly smaller when the shield pipe is used.

The POISSON computation was made for a number of configurations. Septum height, septum recess from the magnet edge, pipe flat spacing from the magnet edge were varied; the effects of chamfering the septum, introducing a slot into the shield pipe, varying the pipe flat geometry were studied. The results ofthese investigations are summarized in the next section.

The OUTPUT.POI output file for a configuration close to that used for the magnet design is given in Appendix I.

5. Conclusions.

1. By using a high-permeability steel beam pipe, one should get smaller fringing fields at the AGS extraction beam than by using a non-magnetic beam pipe. If the beam pipe is not cut too thin at the flat, the beam pipe steel will not saturate magnetically. The Lukens type C-1020 steel appears to be a suitable pipe material. The minimum wall thickness, between the pipe's curved vacuum wall and the flat milled outer surface, should be in the range 0.030" to 0.040". A gap in the range 0.015" to 0.020" between the milled pipe flat and the magnet lamination edge is recommended.

2. As far as practical, the septum conductor should run the full height of the magnet aperture, leaving only the minimal space required for insulation and installation clearance. This will give the best field uniformity within the magnet's main aperture, in the exit beam space, and will minimize leakage flux into the AGS beam tube. When the clearances between the ends of the septum and the magnet laminations are small, the shield pipe will cause little change in the main septum magnet field.

   The outer septum edge should be just at, or slightly inside, the edge of the steel magnet laminations. It sould not protrude outward beyond the lamination edge.

   Chamfering of the magnet lamination edges at the septum produces worse field inhomogeneity and leakage. One should avoid chamfering the lamination edge.

3. Good agreement was obtained with the peak field measurements by E. Rodger and V. Badea [3]. The design chosen by E. Rodger appears near to the optimal available design (as constrained by practical mechanical, vacuum, electrical, and insulation requirements).

   The fringing fields extending into the AGS beam pipe are expected to be acceptably low, when the design using the high permeability beam pipe is used.

4. A procedure for editing the TAPE73.DAT list to eliminate negative area triangles, generated by the LATTICE code, is given in Appendix III.

Acknowledgement

The author wishes to thank Ramesh C. Gupta and John W. Jackson for informative discussions on running the POISSON codes and for the use of Dr. Gupta's improved version of these codes. He wishes to thank E. Rodger and V. Badea for useful discussions on the magnet construction and measurements.

References

1. Los Alamos Accelerator Code Group. Reference Manual For The Poisson/Superfish Group Of Codes. Los Alamos National Laboratory Report LA-UR-87-126, Jan. 1, 1987.

2. Los Alamos Accelerator Code Group. User's Guide For The Poisson/Superfish Group Of Codes. Los Alamos National Laboratory Report LA-UR-87-115, Los Alamos NM 87545, Jan. 1987.

3. E. Rodger and V. Badea, Magnetic Properties of the H-10 Magnet. Booster Technical Note No. 148, Accelerator Development Department, Brookhaven National Laboratory, Upton NY 11973, Sept. 29, 1989.

4. G.E. Fisher, Iron Dominated Magnets. Article in AIP Conference Proceedings No. 153, M. Month and M. Dienes editors, American Institute of Physics, NY, 1987.

5. R.C. Gupta, Improvements in the AUTOMESH and other POISSON Group Codes, Workshop on Electromagnetic Field Computation, Schenectady NY, Oct. 20-21, 1986.

6. R.C. Gupta, Improved Mesh Generator For The POISSON Group Codes, IEEE Proc. NS-34, 1449 (1987).

7. R.L. Keizer, Dipole Septum Magnets. CERN Report PS 74-13, Geneva, May 21,1974.

8. D.W. Bynon and T.C. Shannon, Introduction to VAX/VMS, 2'nd Edition, Professional Press, Inc., Spring House, Penna. 19477.

Appendix I

A Sample Computational Printout

Printouts of the computed field output file OUTPOI.DAT, and the permeability data input file PERM.DAT;21, are given for the computation file SEPTUM.DAT;14 10-13-89 for a configuration close to the magnet design.

The magnet parameters for this calculation are:

Gap (G), at each end of septum, to horizontal lamination edge of magnet, 0.015", Recess, inwards, of septum from vertical lamination edge of magnet, 0.006", A simple flat surface is on the pipe (no raised plateau), Distance from flat pipe surface to vertical lamination edge of magnet, 0.025", Magnet aperture, 1.070", Minimum shield pipe width, 0.0295", Magnet current, 19,560 amperes.

The computed fields at the magnet's horizontal midplane for locations of critical interest are:

	Shield Pipe Inner Wall	Shield Pipe Outer Wall	Septum Outer Edge
Logical K Coordinate	67	70	71
X Position (Milli-inches)	-54.5	-25.0	+6.0
H_y (Oersted)	-4.44	-17.83	-18.55
μ_{rel}	1,235	740	1.00
$\|B\|$ Gauss	5,490	13,200	18.55

The B-field amplitudes just within the steel pipe wall, listed in the last column, are not large enough to saturate the pipe magnetically.

Appendix II

Running POISSON Codes On The BNL VAX Computers

The general description and operation of the POISSON codes appear in the Los Alamos User's Guide and Los Alamos Reference Manual for the Poisson/Superfish Group of Codes [1,2]. In this Appendix we list commands used to run these codes on the BNL VAX computers and get printed output data and graphics on the AGS Department's LZ911 laser printer. Graphics output from the TEKPLOT code is viewed interactively on a Digital Equipment Corporation type VT240 monitor screen. The codes are run on the VAX Cluster-6 machine, and output files are transferred to the BNLDAG machine to allow printout on the laser printer. An allotted "disk quota" of 10,000 blocks of 512-byte VAX virtual memory was required for convergence of the H-10 magnet Poisson calculations.

The commands for running the BNL-modified POISSON codes are:

```
RUN $2$DUA3:[GUPTA.BNL]AUTOBNL
RUN $2$DUA3:[GUPTA.BNL]LATBNL
RUN $2$DUA3:[GUPTA.BNL]POISBNL
RUN $2$DUA3:[GUPTA.BNL]TEKP_DISSPLAS .
```

Before the POISSON and TEKPLOT codes can be run, they must be activated by use of the commands

PUB POISSON and
PUB DISSPLAS, respectively.

When computations are to be made for magnets containing materials of variable permeability one requires a data file containing the permeability data information. The construction of such files is explained in the LANL manuals. (The file PERM.DAT;21 used in the H-10 magnet computations is included in this note, as an example). When the POISSON code is run, the program will interactively request the permeability file as an input data file. When the name of the permeability file is entered, as the requested input file, the running of the POISSON code will commence. At the completion of the run, the calculation output results will be stored in the file OUTPOI.LIS;1 . The contents of this file can be printed at the AGS laser printer by use of the commands:

COPY OUTPOI.LIS;1

(To:)

BNLDAG::LZ911:OUTPOI.LIS;1.

To interactively run the TEKPLOT graphics codes enter the commands:

PUB POISSON

PUB DISSPLAS

RUN 2DUA3:[GUPTA.BNL]TEKP_DISSPLAS.

If a Digital Equipment Corporation type VT240 video monitor is available, the graphics generation can be viewed on the monitor screen by interactively answering the program request for a plot device with the reply PLOT DEVICE=VT240. A graphics printout file TALARIS.LIS;1 will be generated, instead, if one enters the reply PLOT DEVICE = TALARIS.

If a D.E.C. type VT220 terminal is used, the TEKPLOT code can be run interactively, but the graphics can not be viewed from the monitor screen. When this type of terminal is used, use the response PLOT DEVICE = TALARIS to generate the graphics output file TALARIS.LIS;1.

To print out graphics on the LZ911 printer one must first transfer the graphics output file to the BNLDAG VAX computer. This is accomplished by entering the command:

COPY TALARIS.LIS;1 BNLDAG"username password"::DUA3:[username].

Control of the user's keyboard is then temporarily transferred to the BNLDAG machine by use of the command SET HOST and responding interactively to requests for node, user, and password by the replies BNLDAG, and the user name and password in sequence. The graphics output file is then printed by entering the command:

$ PRINT/FORM=TEK/QUE=LZ911Q TALARIS.LIS;1 .

In practice, the amount of typing required to run the commands and programs above can be reduced by defining a lexical command file containing abbreviated names of these commands and programs.

As an aid to inspect the lattice structure generated by the TAPE73.DAT and LATTICE codes, and as a tool to modify the input data of TAPE73.DAT, the triangular grid diagram illustrated in Figure 14 has proved to be useful. The grid sheet should be used with the dot at the lower left corner.

Appendix III

Correction Of LATTICE Code Input Data For Elimination Of Negative Area Triangles

If negative area triangles are generated while running the LATTICE code, then POISSON will not run to completion. The locations of these triangles will appear on the monitor screen during the running of the code. The triangular lattice generated by LATTICE can be printed out by using the TEKPLOT code, and inspected visually for improper lattice points.

Each proper vertex point of the lattice will be joined to six distinct vertex points of a hexagonal cell which surrounds this vertex point. Improper lattice points will not be surrounded by a hexagonal cell. Furthermore, the improper lattice points will occur as directly-linked pairs, each linked pair lying on a boundary polygon separating two of the computational regions specified by the TAPE73.DAT input data code.

The lattice can be reconfigured to a proper lattice by the following procedure. For each pair of improper lattice points directly linked by a boundary path segment, select one point of the pair. Remove all triangle sides joining the selected point to other lattice points, except for those sides which lie on the boundary path; slide the selected point onto the other point of the pair. Then slide the point further, onto an adjoining non-boundary triangle side, and join a connecting segment to each of the six points surrounding it. It is easy to implement this procedure! For each pair of improper lattice points, located by inspecting the TEKPLOT lattice diagram: remove one point of the pair from the list of boundary points in file TAPE73.DAT, by deleting the coordinates K,L,x,y of this point. Then replace the x,y coordinates of the other point by those of the deleted point or leave them unchanged, according to which choice results in a more uniform lattice. When the LATTICE code is rerun, using the amended TAPE73.DAT input data file, the lattice generated will be free of negative area triangles.

The correction is illustrated in Figures 12 and 13. In Fig. 12 the TEKPLOT printout of a LATTICE computation is shown, which has negative area triangles in five locations; a reconfiguration which eliminates these triangles is generated in Fig. 13. To do the correction in practice, one needs simply to delete the hollow circled points from the data points in TAPE73.DAT, and rerun the LATTICE code.

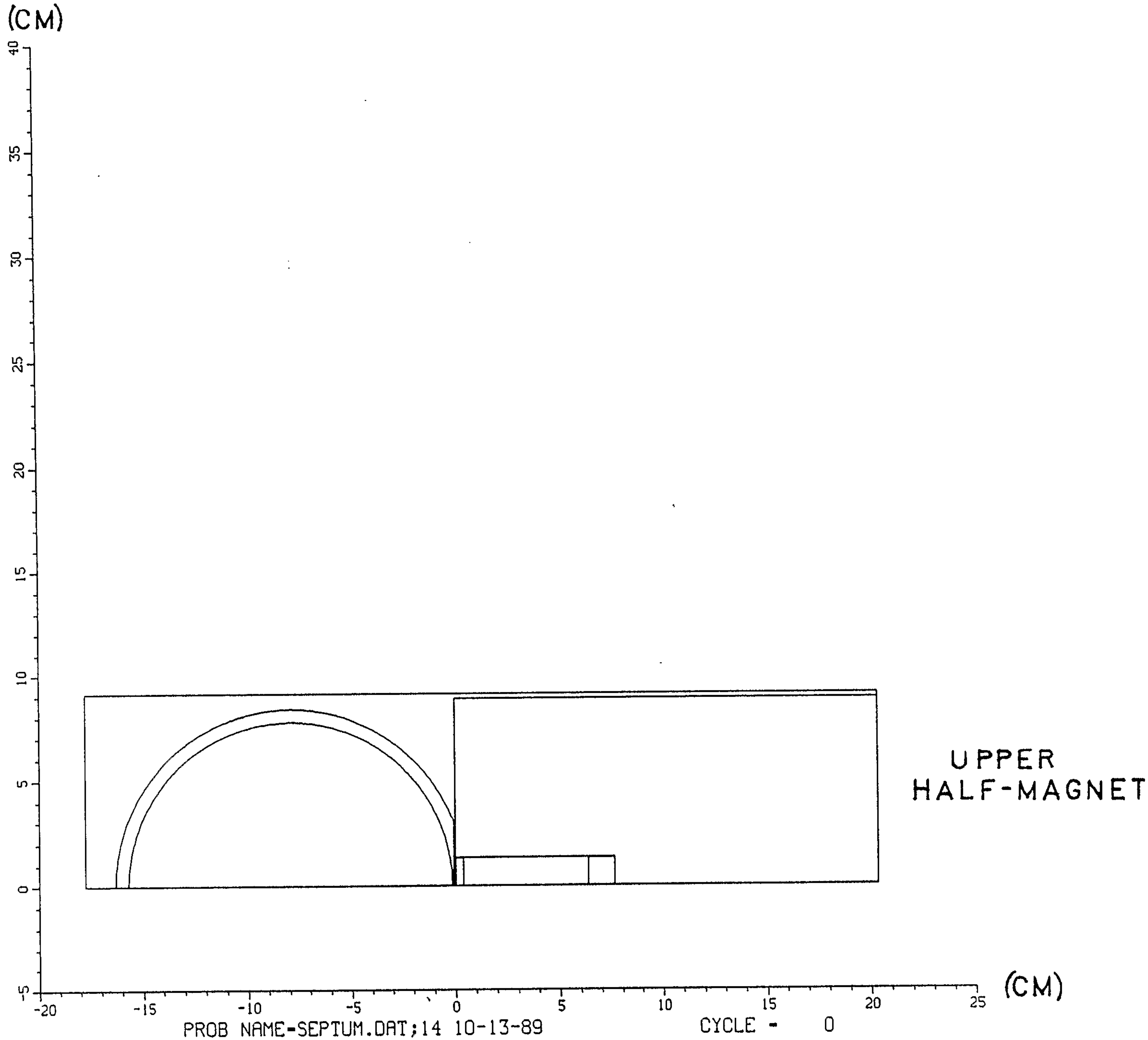

FIG. 1 THE H-10 SEPTUM MAGNET GEOMETRY

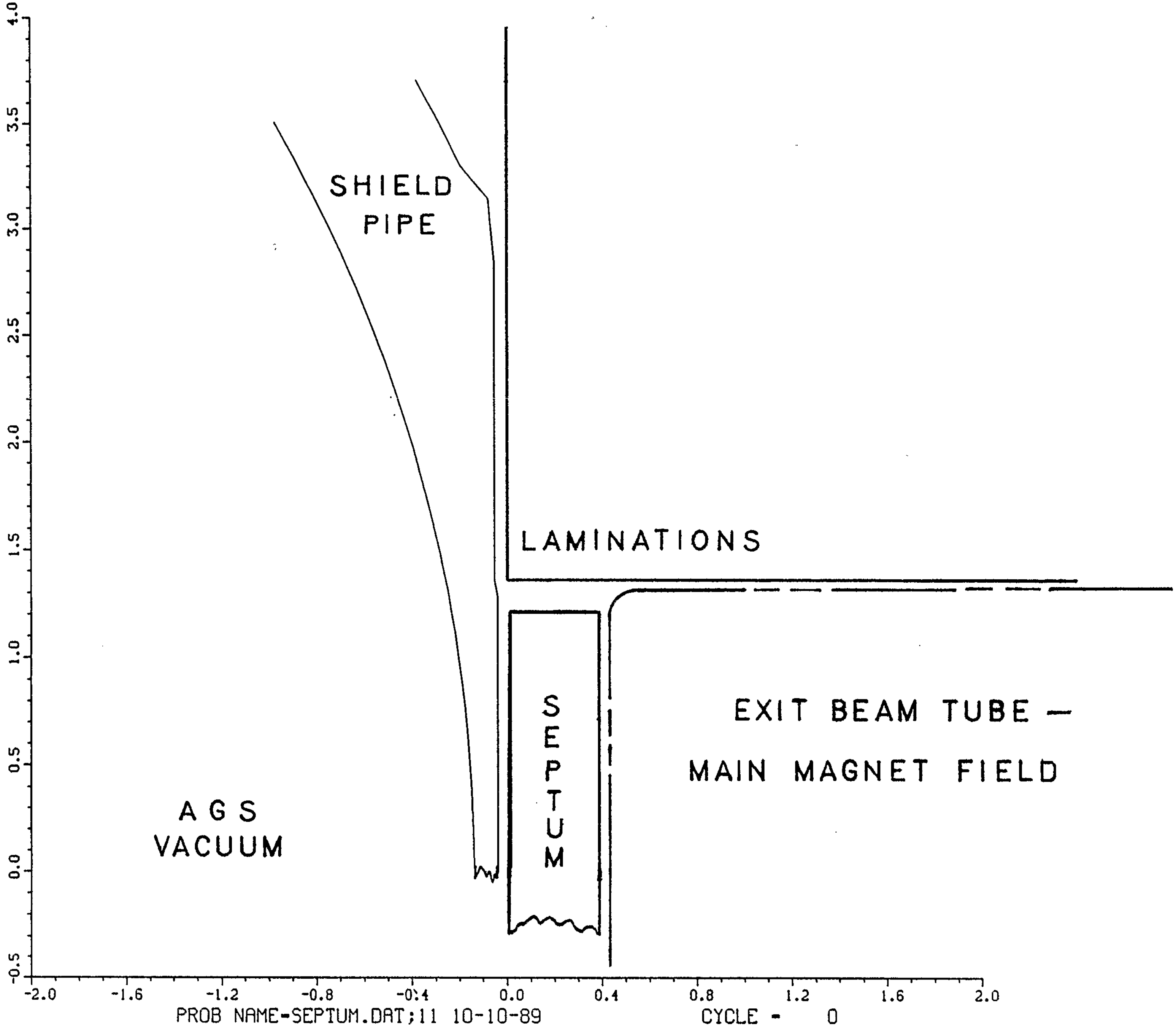

FIG.2 THE REGION BETWEEN PIPE AND SEPTUM

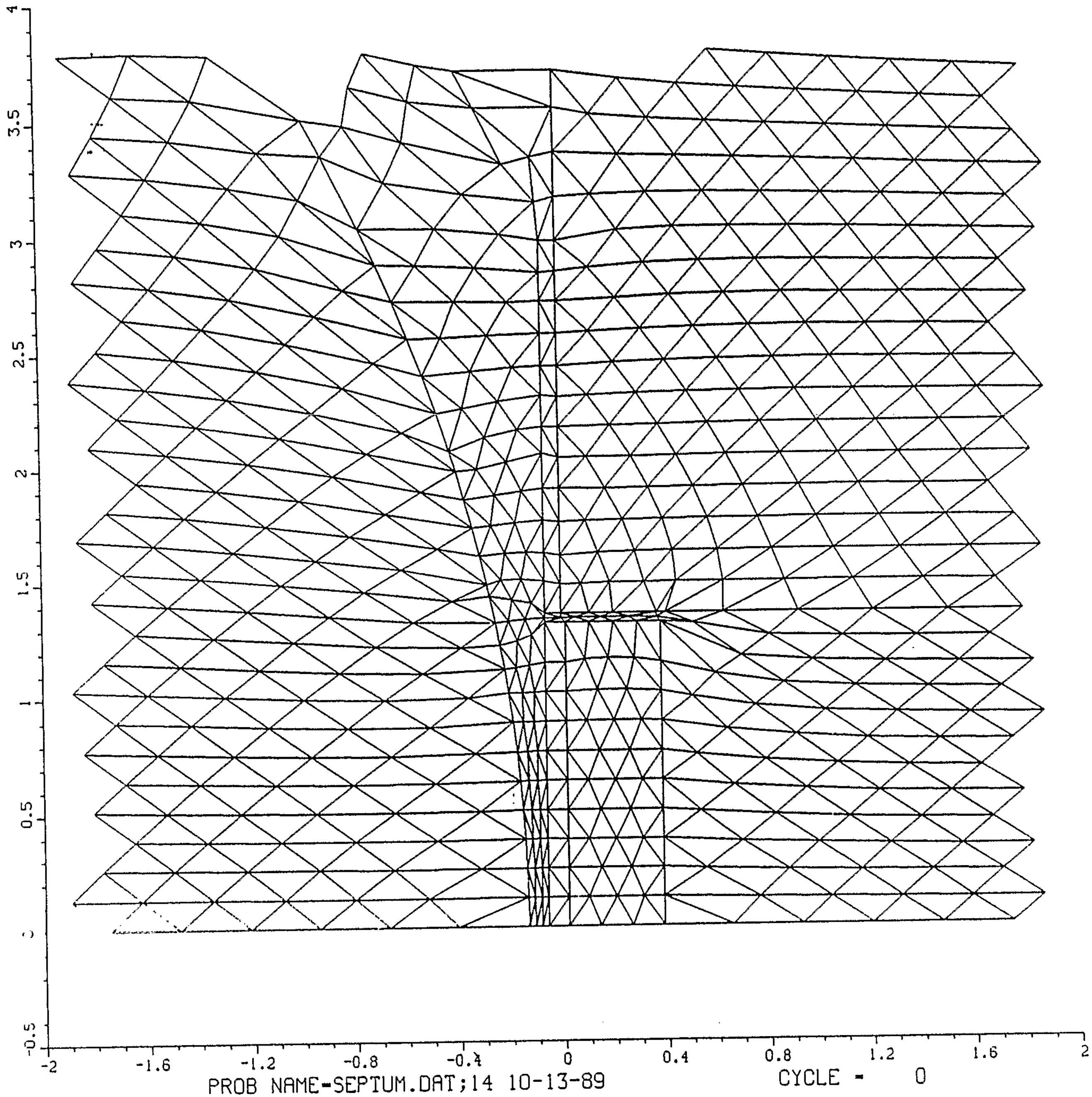

FIG. 3 COMPUTATIONAL LATTICE NEAR THE SEPTUM

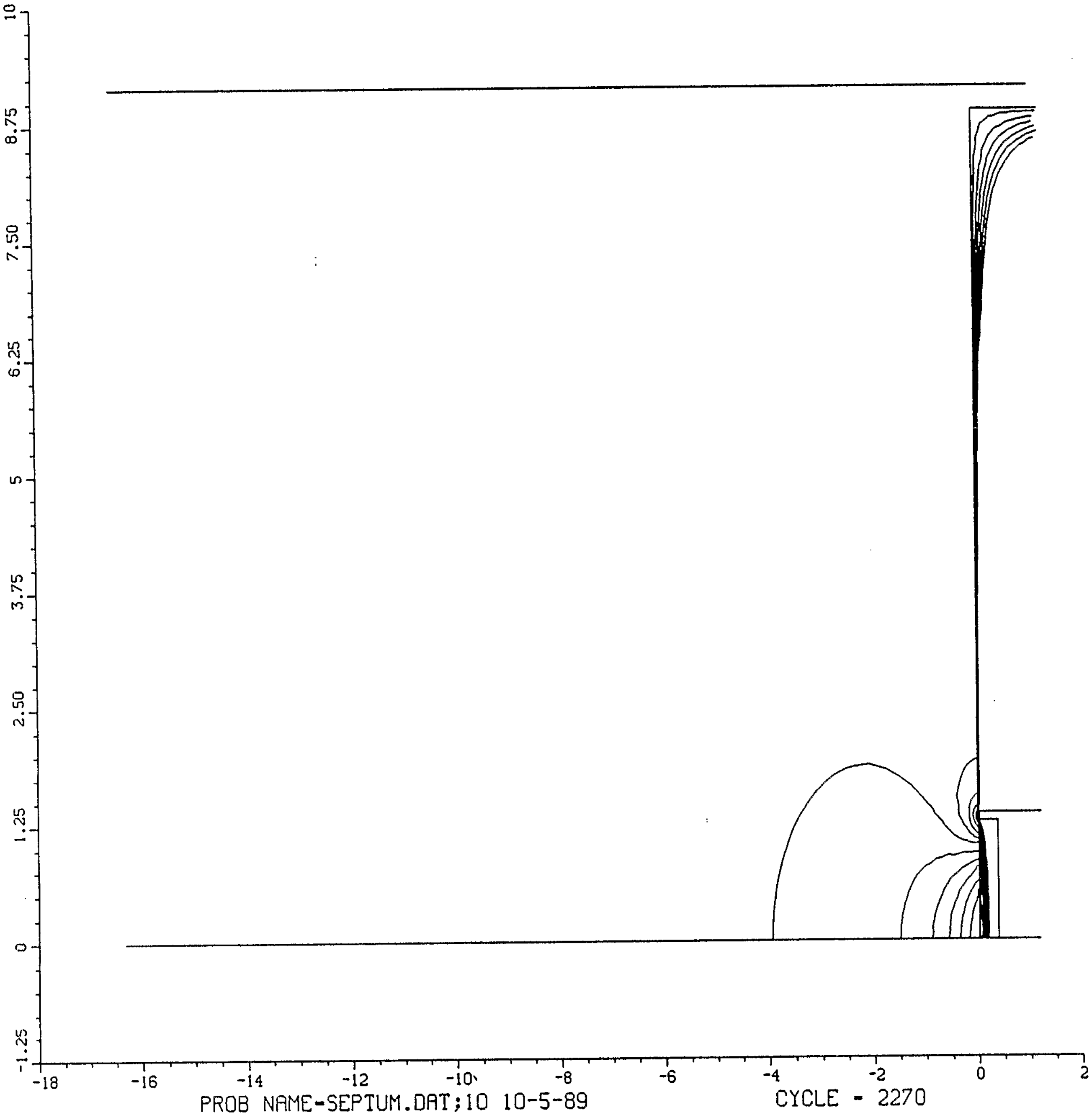

FIG. 4 MAGNETIC EQUIPOTENTIAL LINES - NO SHIELD PIPE

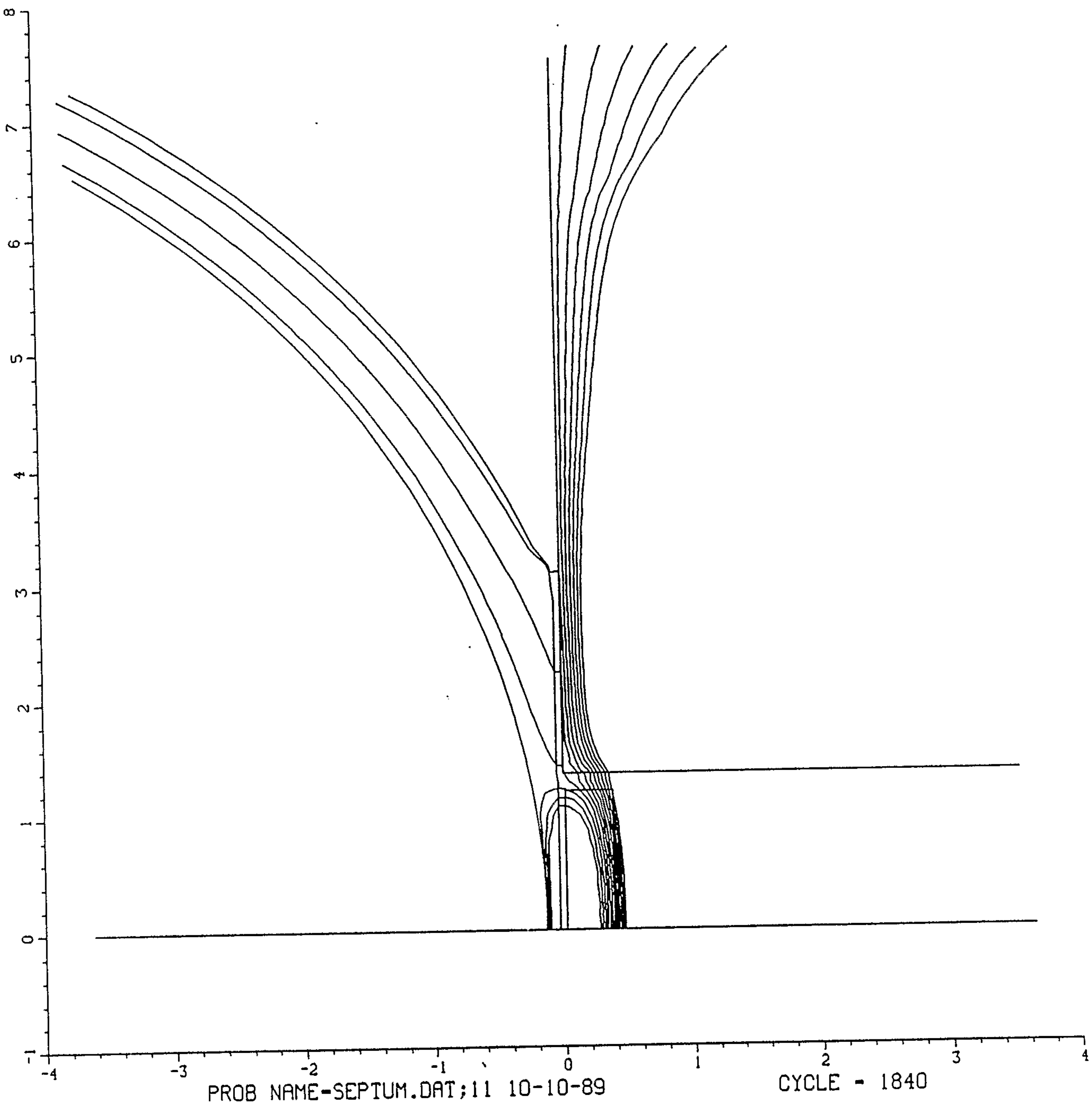

FIG. 5 EQUIPOTENTIAL LINES - WITH SHIELD PIPE

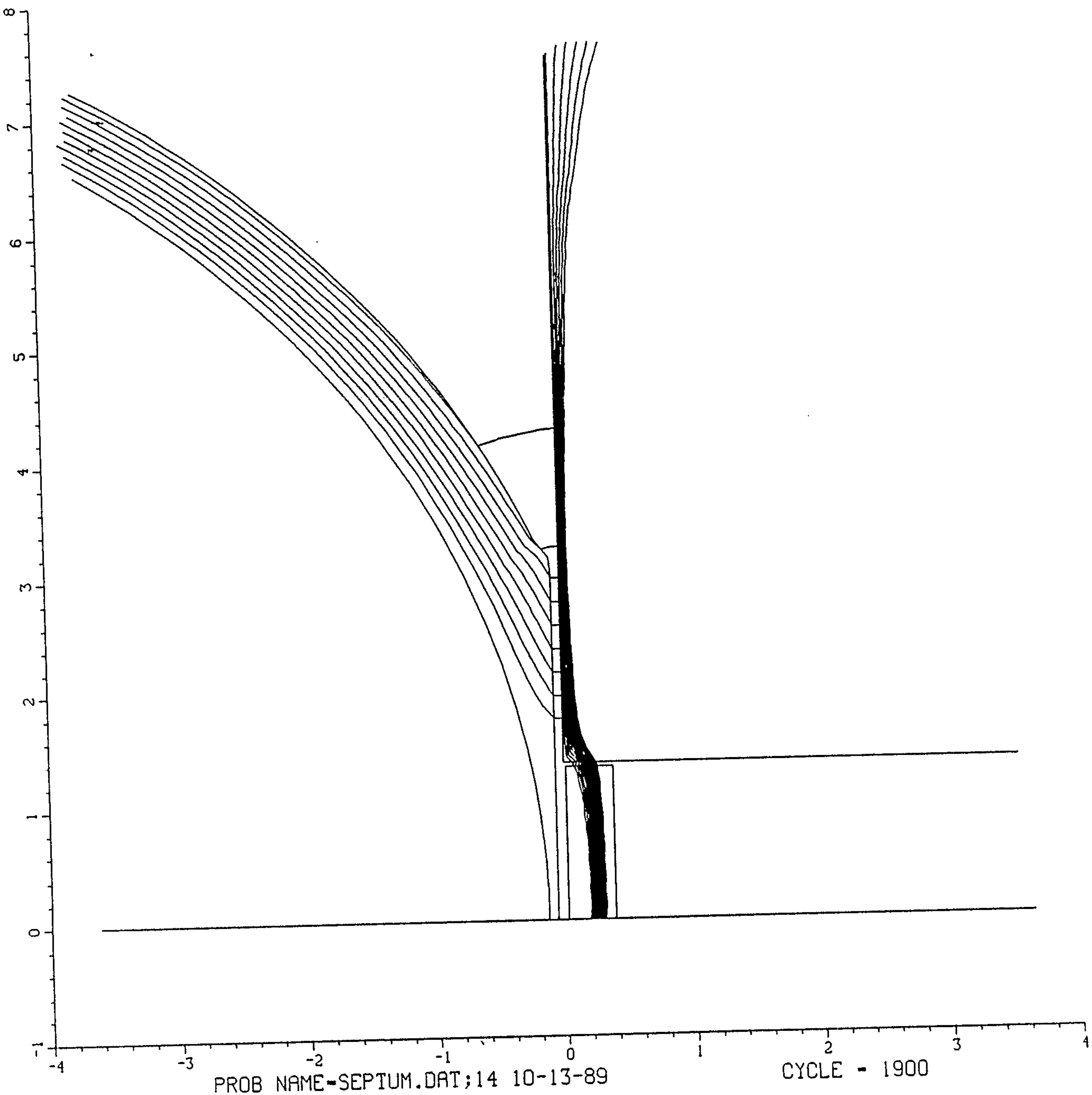

8
7
6
5
4
3
2
1
0
-1
-4
-3
-2
-1
0
1
2
3
4
PROB NAME-SEPTUM.DAT;14 10-13-89
CYCLE - 1900

FIG. 6

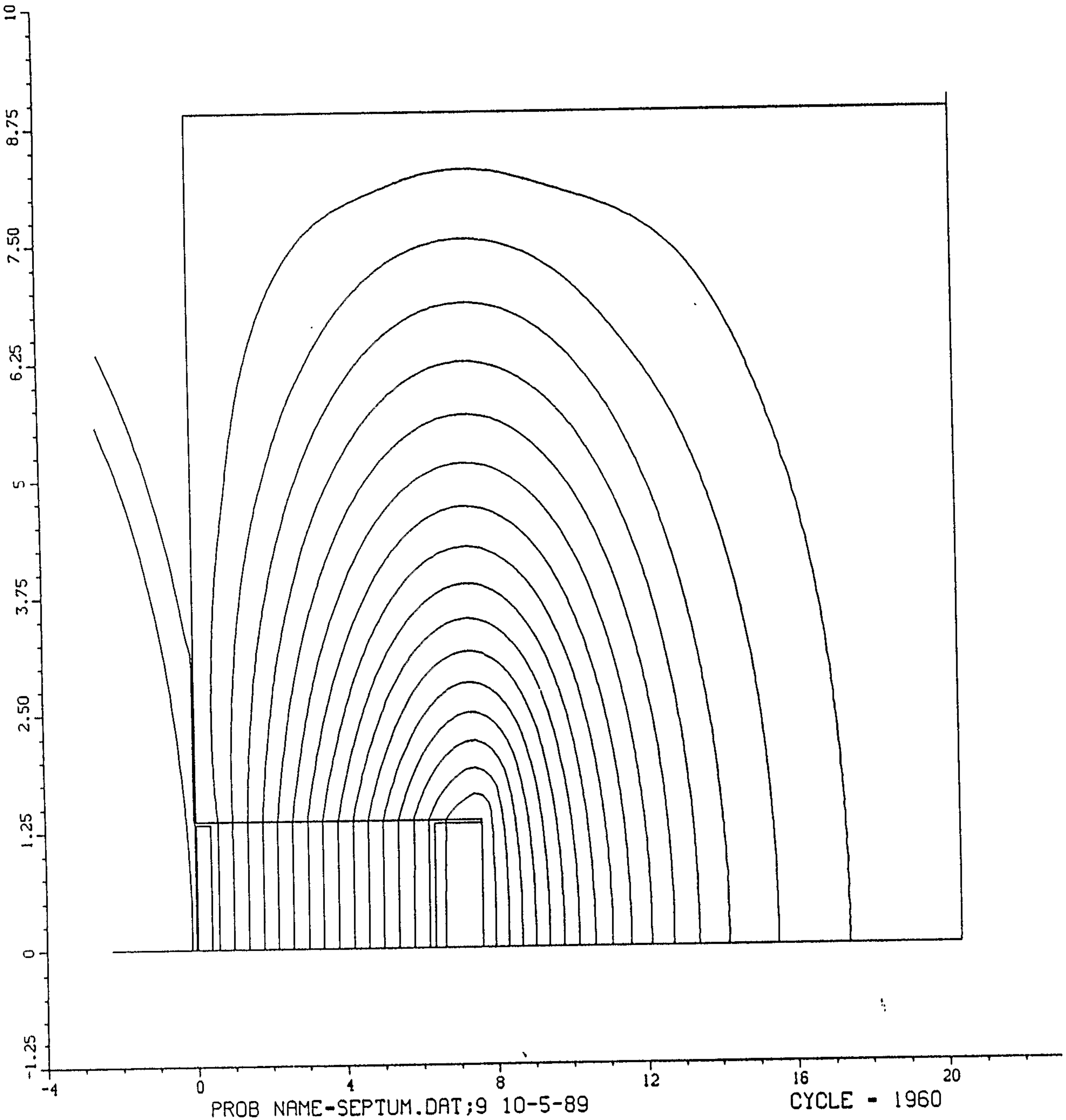
10
8.75
7.50
6.25
5
3.75
2.50
1.25
0
-1.25
-4
0
4
8
12
16
20
PROB NAME-SEPTUM.DAT;9 10-5-89
CYCLE - 1960

FIG. 7

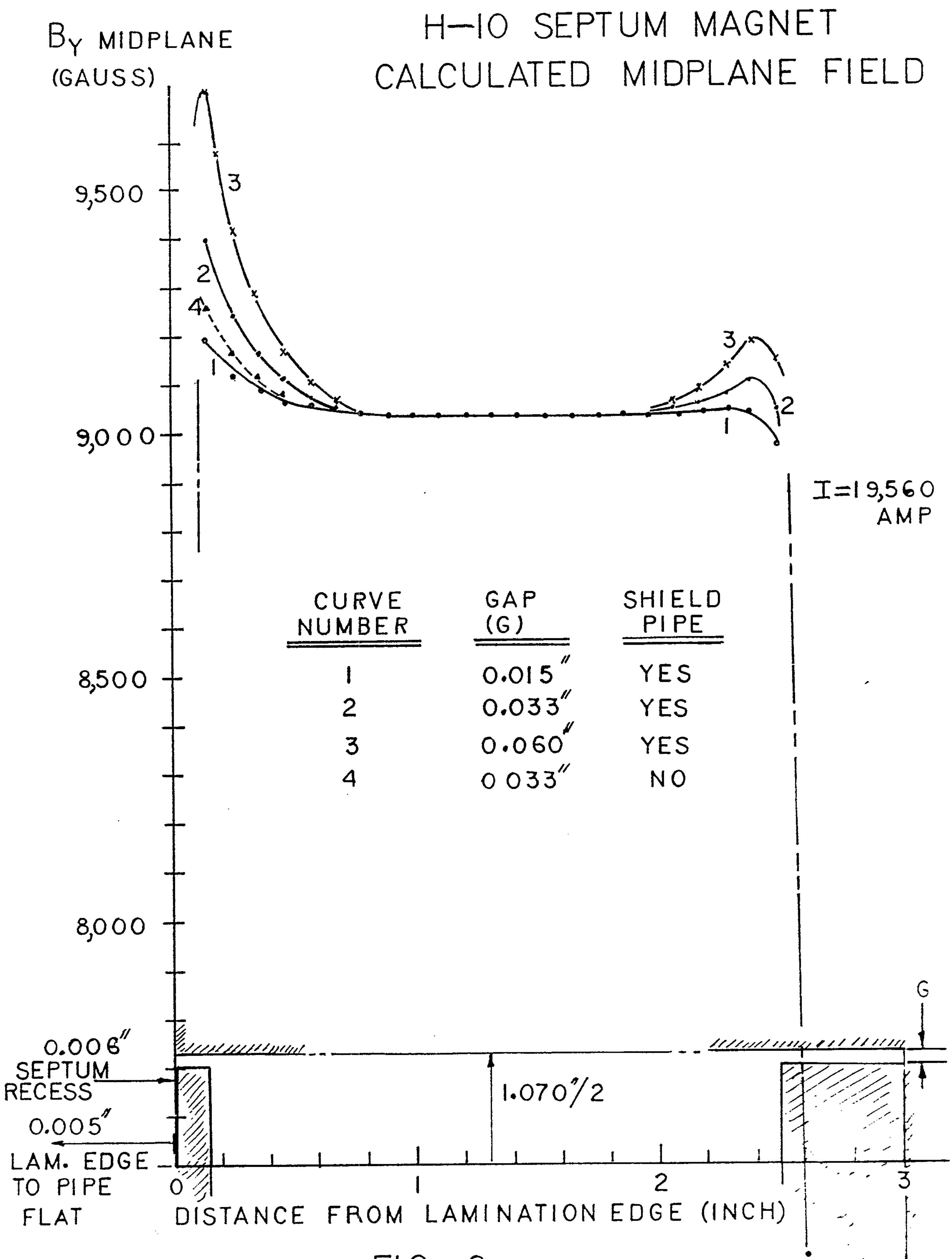

H-10 SEPTUM MAGNET
CALCULATED MIDPLANE FIELD
BY MIDPLANE (GAUSS)
9,500
9,000
8,500
8,000
I=19,560 AMP
CURVE NUMBER
GAP (G)
SHIELD PIPE
1 0.015″ YES
2 0.033″ YES
3 0.060″ YES
4 0.033″ NO
0.006″ SEPTUM RECESS
0.005″
LAM. EDGE TO PIPE FLAT
1.070″/2
G
0
1
2
3
DISTANCE FROM LAMINATION EDGE (INCH)

FIG. 8

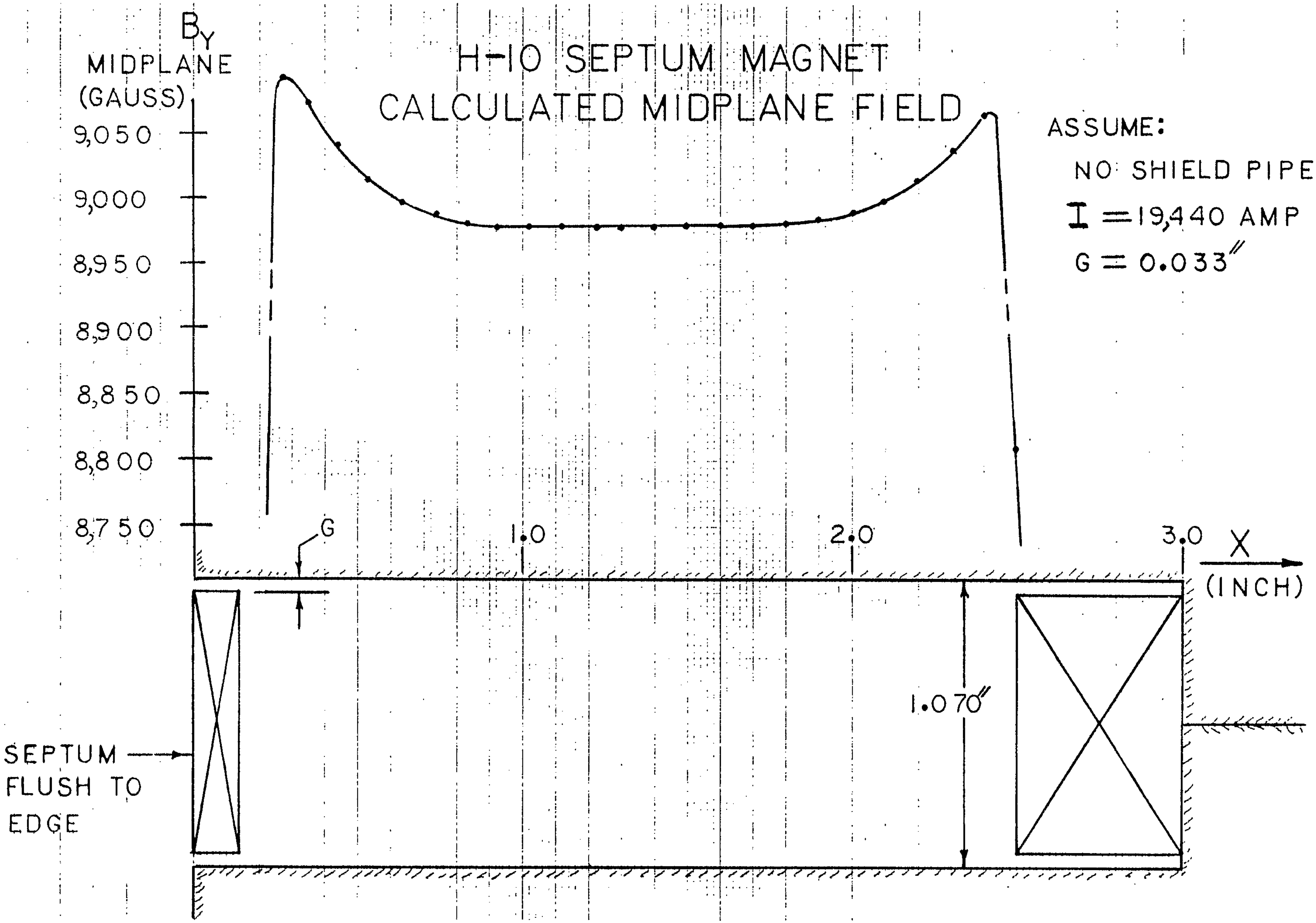
H-10 SEPTUM MAGNET
CALCULATED MIDPLANE FIELD
B_Y
MIDPLANE
(GAUSS)
9,050
9,000
8,950
8,900
8,850
8,800
8,750
G
1.0
2.0
3.0
X
(INCH)
ASSUME:
NO SHIELD PIPE
I = 19,440 AMP
G = 0.033″
1.070″
SEPTUM
FLUSH TO
EDGE

FIG. 9

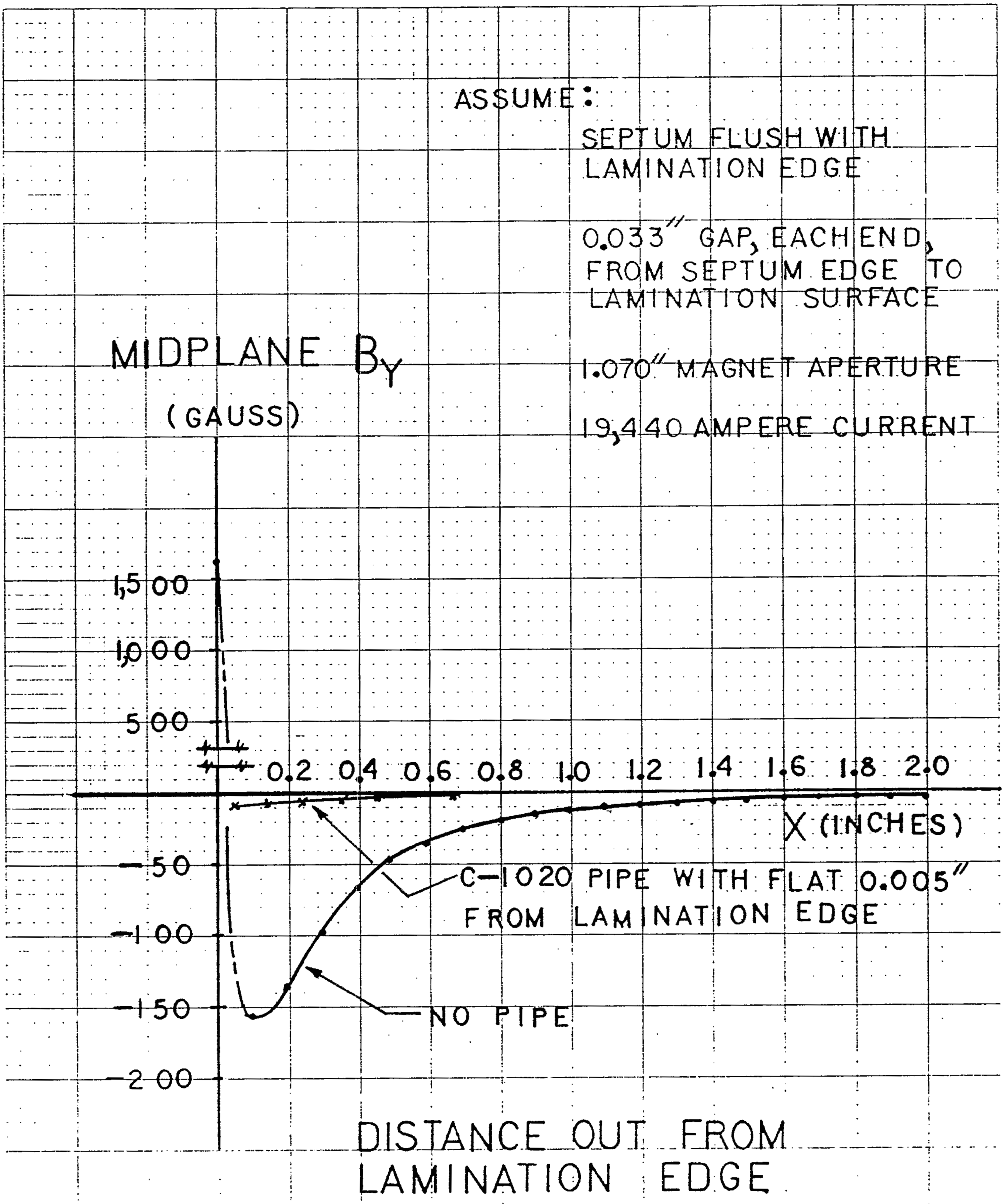

H−10 SEPTUM MAGNET
CALCULATED STRAY FIELD

FIG. 10

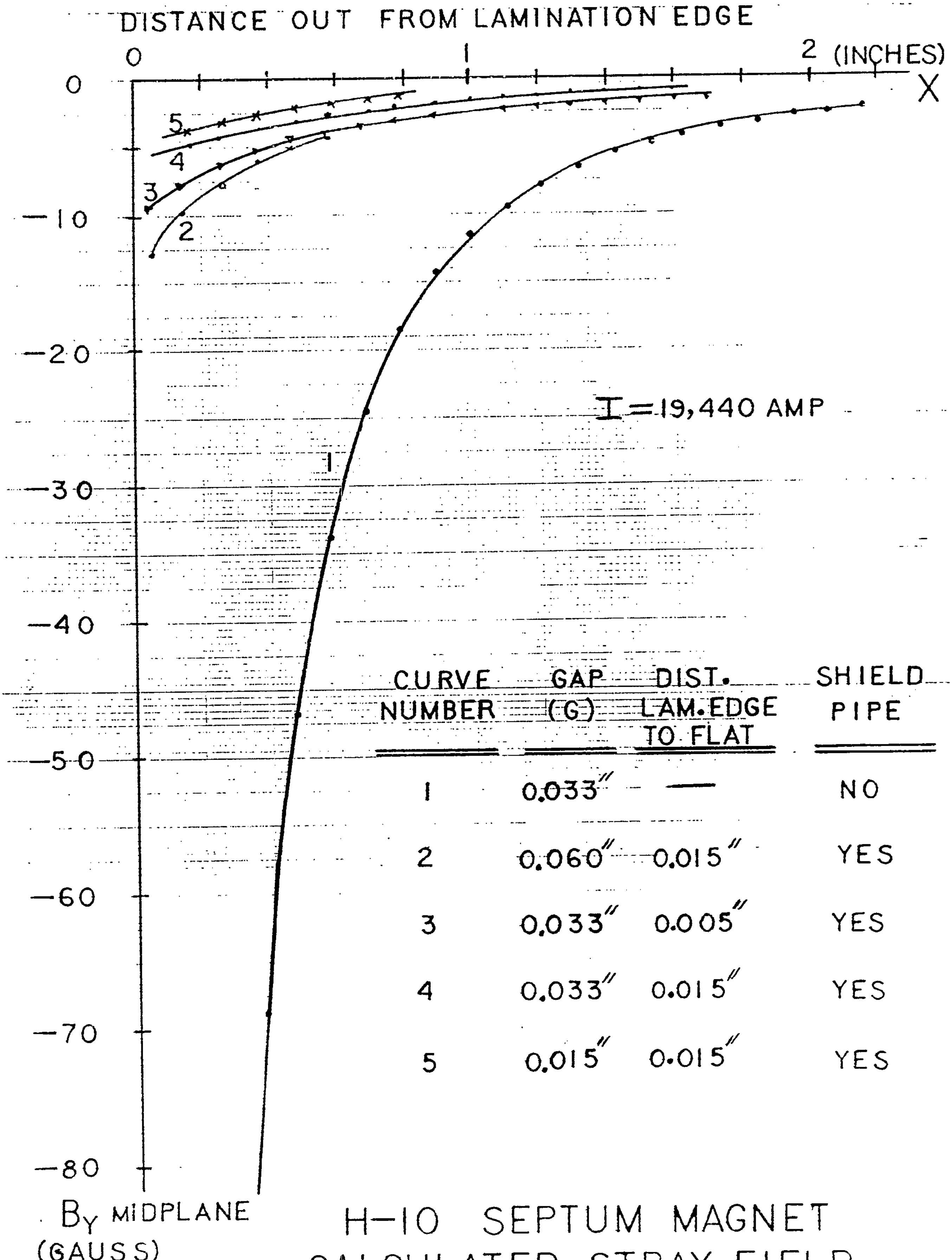

CURVE NUMBER	GAP (G)	DIST. LAM. EDGE TO FLAT	SHIELD PIPE
1	0.033″	—	NO
2	0.060″	0.015″	YES
3	0.033″	0.005″	YES
4	0.033″	0.015″	YES
5	0.015″	0.015″	YES

H-10 SEPTUM MAGNET
CALCULATED STRAY FIELD

FIG. 11

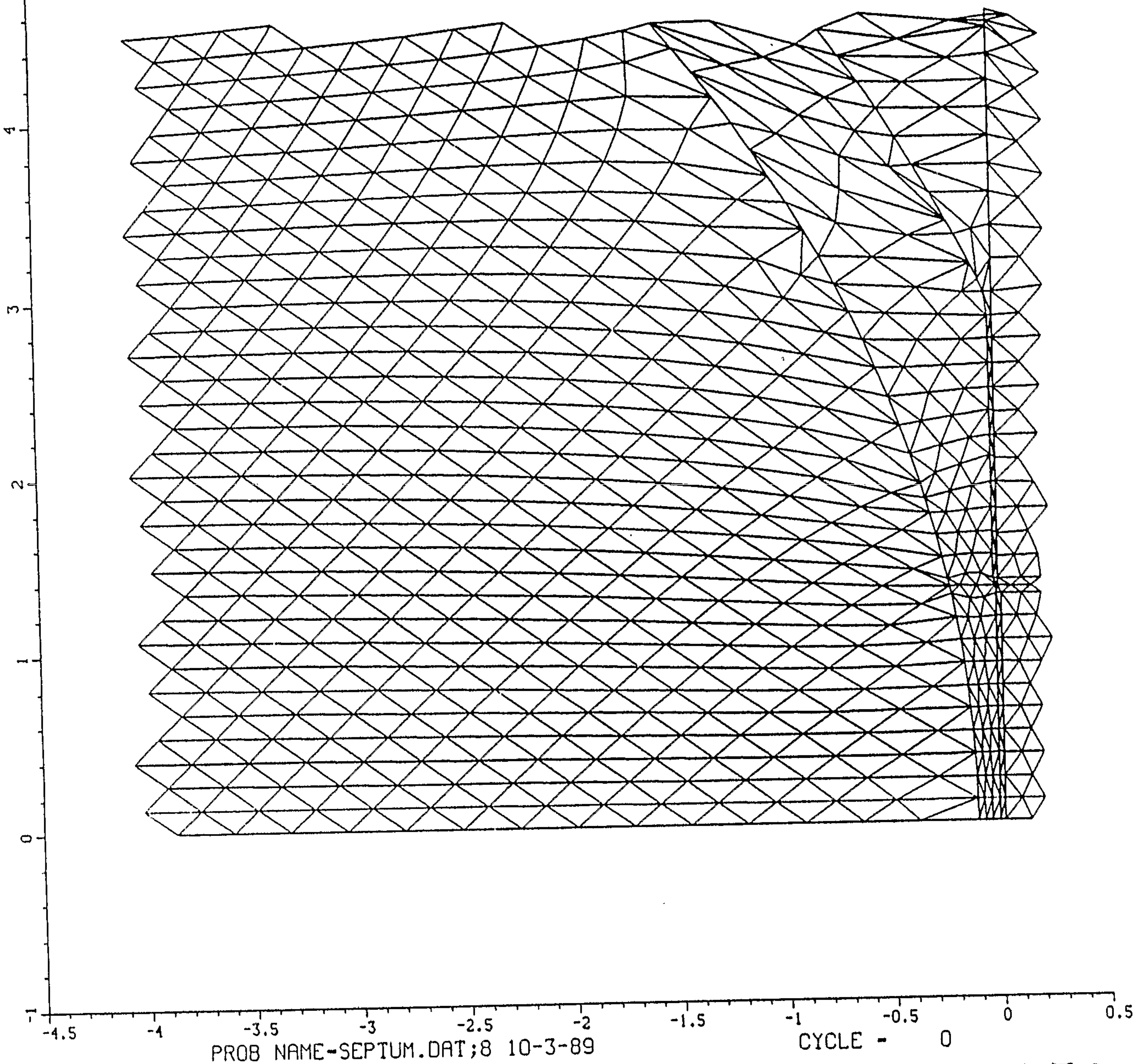

FIG. 12 LATTICE WITH NEGATIVE AREA TRIANGLES

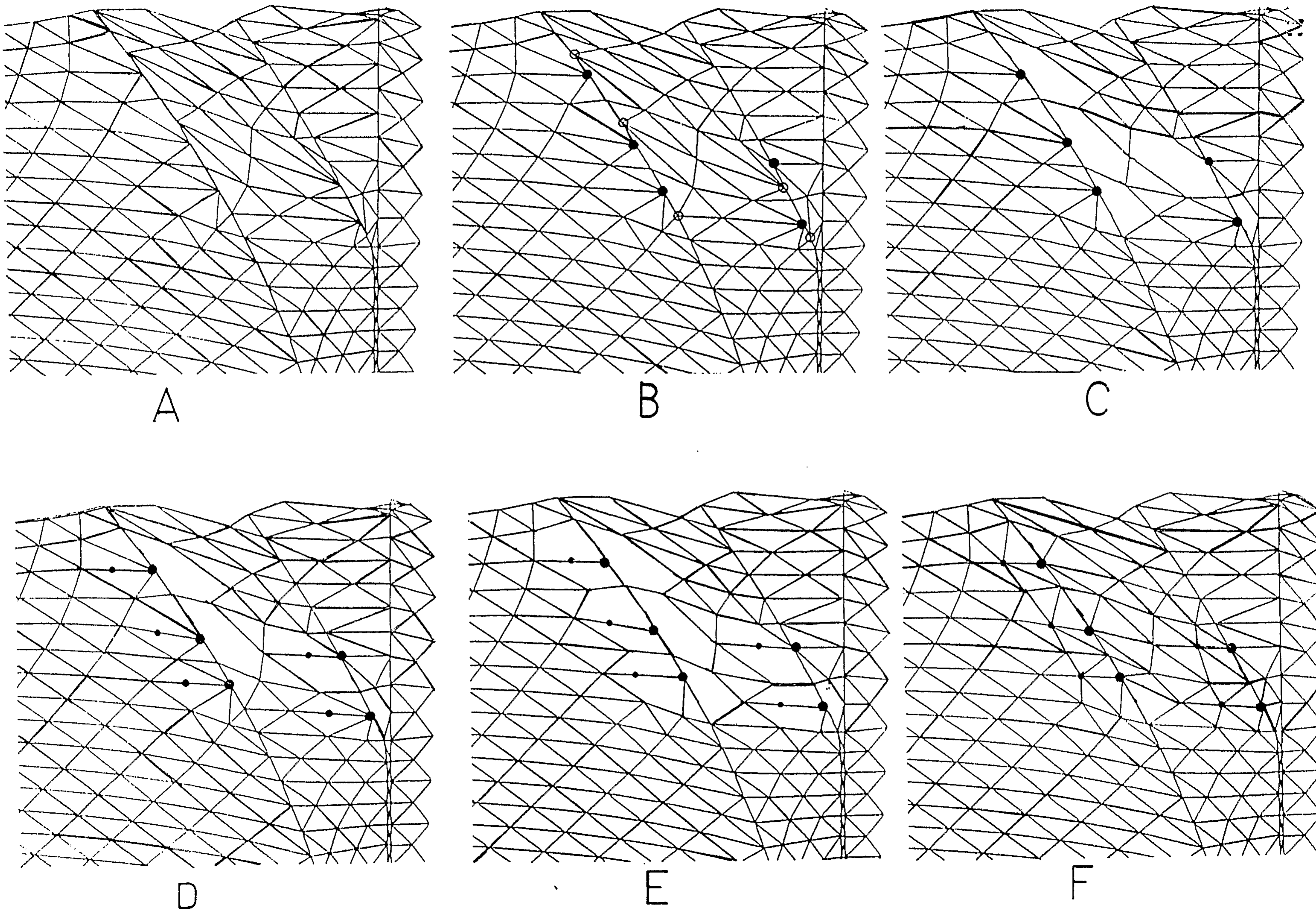

FIG. 13 REMOVAL OF NEGATIVE AREA TRIANGLES

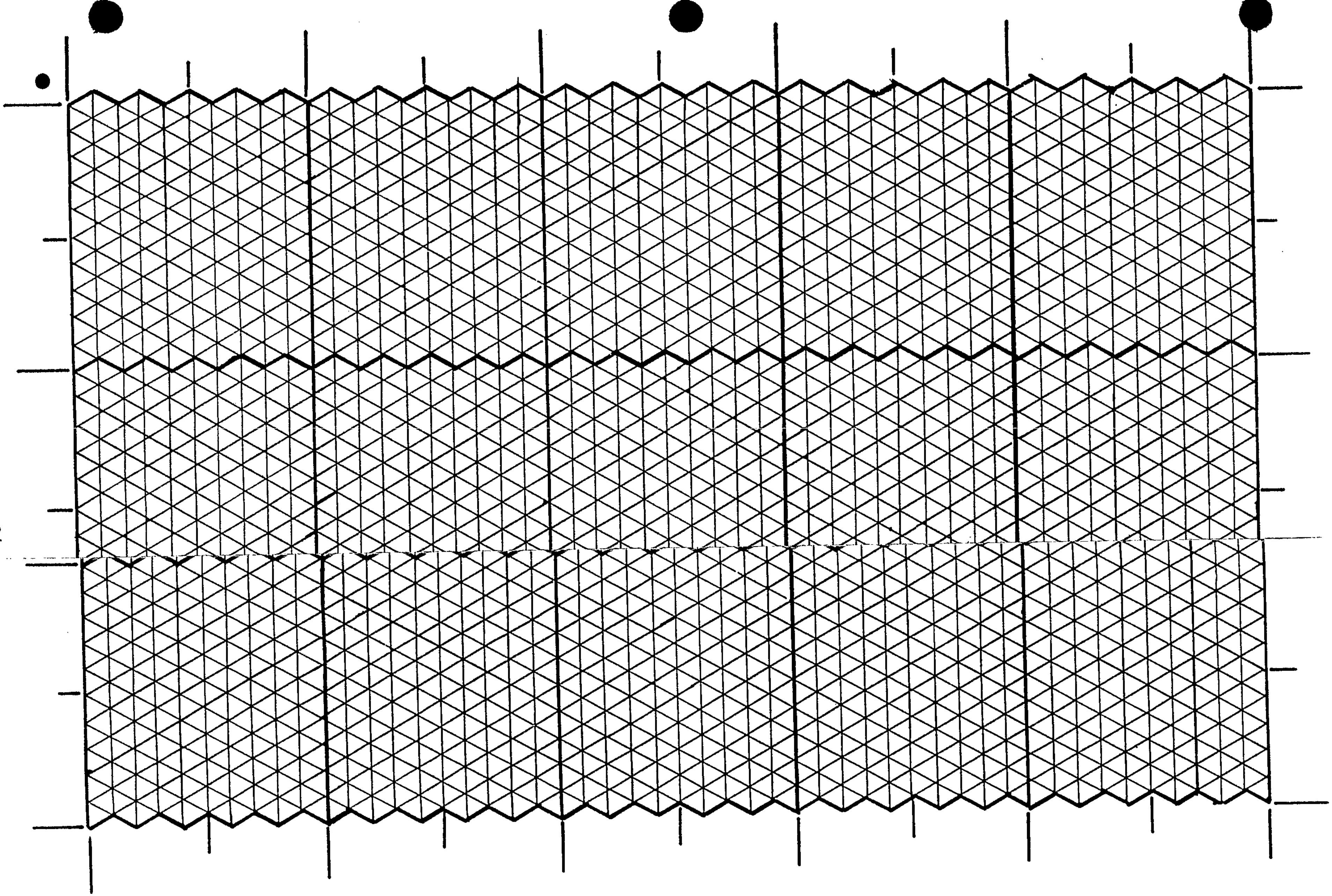

FIG. 14

N	B-SQUARED	B(GAUSS)	GAMMA	MU	H(OERSTEAD)	D-GAM/D-B	D-GAM/D-BSQ
1	4.000000E+04	200.00	0.000500	2000.00	0.10	0.0000E+00	0.0000E+00
2	1.600000E+05	400.00	0.000500	2000.00	0.20	3.0303E-07	3.1898E-10
3	3.025000E+05	550.00	0.000545	1833.33	0.30	-3.1702E-07	-1.7136E-10
4	1.690000E+06	1300.00	0.000308	3250.00	0.40	-8.2418E-08	-2.4975E-11
5	4.000000E+06	2000.00	0.000250	4000.00	0.50	-3.6550E-08	-6.3017E-12
6	1.444000E+07	3800.00	0.000184	5428.57	0.70	-1.0754E-08	-1.0543E-12
7	4.096001E+07	6400.00	0.000156	6400.00	1.00	4.0064E-09	2.6016E-13
8	8.100000E+07	9000.00	0.000167	6000.00	1.50	1.8315E-08	9.4407E-13
9	1.081600E+08	10400.00	0.000192	5200.00	2.00	3.8633E-08	1.7886E-12
10	1.254400E+08	11200.00	0.000223	4480.00	2.50	3.3482E-08	1.4432E-12
11	1.440000E+08	12000.00	0.000250	4000.00	3.00	9.2801E-08	3.7571E-12
12	1.612900E+08	12700.00	0.000315	3175.00	4.00	1.2765E-07	4.9287E-12
13	1.742400E+08	13200.00	0.000379	2640.00	5.00	3.3980E-07	1.2679E-11
14	1.849600E+08	13600.00	0.000515	1942.86	7.00	5.8473E-07	2.0445E-11
15	2.250000E+08	15000.00	0.001333	750.00	20.00	1.7917E-06	5.7796E-11
16	2.560000E+08	16000.00	0.003125	320.00	50.00	3.1024E-06	9.4298E-11
17	2.856101E+08	16900.00	0.005917	169.00	100.00	4.7278E-06	1.2847E-10
18	3.960101E+08	19900.00	0.020101	49.75	400.00	3.1085E-05	7.6376E-10
19	4.326400E+08	20800.00	0.048077	20.80	1000.00	5.7442E-05	1.3990E-09<----(These Slopes are Estimated)

RECONSTRUCTION OF THE TABLE FOR MAT. NO. 4 WITH EQUAL INCREMENTS OF B-SQUARED

MAXIMUM B-SQUARED = 4.326400E+08, WITH EXTRAPOLATION OR TRUNCATION FOR HIGHER VALUES
(Truncation is used for MODE (PROB CON 6) = 1, and Extrapolation for MODE = 0)

B-SQUARED INCREMENT = 1.081589E+06

B-SQUARE GAMMA TABLE IS CONSTRUCTED USING CUBIC SPLINE IN B AND GAMMA.

MATERIAL NO.[illegible], STACK=1.000 LUKENS C-1020 MEDIUM CARBON STEEL

N	B-SQUARED	B(GAUSS)	GAMMA	MU	H(OERSTEAD)	D-GAM/D-B	D-GAM/D-BSQ
1	1.000000E+06	1000.00	0.001754	570.13	1.75	-5.0400E-07	-1.6800E-10
2	4.000000E+06	2000.00	0.001250	800.00	2.50	-2.4000E-07	-4.8000E-11
3	9.000000E+06	3000.00	0.001010	990.10	3.03	-1.2270E-07	-1.7529E-11
4	1.600000E+07	4000.00	0.000887	1127.01	3.55	-6.4260E-08	-7.1400E-12
5	2.500000E+07	5000.00	0.000823	1215.01	4.12	-3.4440E-08	-3.1309E-12
6	3.600000E+07	6000.00	0.000789	1268.07	4.73	-7.3500E-09	-5.6538E-13
7	4.900000E+07	7000.00	0.000781	1280.00	5.47	1.4250E-08	9.5000E-13
8	6.400000E+07	8000.00	0.000796	1257.07	6.36	4.4830E-08	2.6371E-12
9	8.100000E+07	9000.00	0.000840	1190.01	7.56	6.8760E-08	3.6189E-12
10	1.000000E+08	10000.00	0.000909	1100.00	9.09	1.0301E-07	4.9052E-12
11	1.210000E+08	11000.00	0.001012	988.04	11.13	1.3460E-07	5.8522E-12
12	1.440000E+08	12000.00	0.001147	872.07	13.76	2.1190E-07	8.4760E-12
13	1.690000E+08	13000.00	0.001359	736.05	17.66	3.5080E-07	1.2993E-11
14	1.960000E+08	14000.00	0.001709	585.00	23.93	5.6330E-07	1.9424E-11
15	2.250000E+08	15000.00	0.002273	440.01	34.09	8.5230E-07	2.7494E-11
16	2.560000E+08	16000.00	0.003125	320.00	50.00	1.3194E-06	3.9982E-11
17	2.890001E+08	17000.00	0.004444	225.00	75.55	2.5486E-06	7.2817E-11
18	3.240000E+08	18000.00	0.006993	143.00	125.87	4.1180E-06	1.1130E-10
19	3.610001E+08	19000.00	0.011111	90.00	211.11	1.2209E-05	1.0259E-10
20	1.000000E+10	100000.00	1.000000	1.00	100000.00	2.0299E-05	9.3888E-11<----(These Slopes are Estimated)

RECONSTRUCTION OF THE TABLE FOR MAT. NO. 3 WITH EQUAL INCREMENTS OF B-SQUARED

MAXIMUM B-SQUARED = 1.000000E+10, WITH EXTRAPOLATION OR TRUNCATION FOR HIGHER VALUES
(Truncation is used for MODE (PROB CON 6) = 1, and Extrapolation for MODE = 0)

B-SQUARED INCREMENT = 2.499975E+07

B-SQUARE GAMMA TABLE IS CONSTRUCTED USING CUBIC SPLINE IN B AND GAMMA.

LEAST SQUARES EDIT OF PROBLEM , CYCLE 1900

MIDPLANE SYMMETRY TYPE

STORED ENERGY = 2.87093E+02 JOULES / METER OR RADIAN

XJFACT= 1.000000

SEPTUM.DAT;14 / OUTPUT.DAT

PARAMETERS LISTED IN APPENDIX I.

17,360 AMPERES

27

K	L	A(VECTOR)	X (INCHES)	Y (INCHES)	BX(GAUSS)	BY(GAUSS)	BT(GAUSS)	DBY/DY(GAUSS/CM)	DBY/DX(GAUSS/CM)	AFIT
1	1	0.000000E+00	-7.00000	0.00000	0.000	-1.364	1.364	0.0000E+00	-1.5668E-04	1.4E-06
2	1	3.987243E-01	-6.88490	0.00000	0.000	-1.364	1.364	0.0000E+00	-1.8120E-03	2.2E-05
3	1	7.976128E-01	-6.76980	0.00000	0.000	-1.365	1.365	0.0000E+00	-3.7470E-03	4.8E-05
4	1	1.196775E+00	-6.65470	0.00000	0.000	-1.366	1.366	0.0000E+00	-5.2160E-03	1.2E-04
5	1	1.596256E+00	-6.53960	0.00000	0.000	-1.367	1.367	0.0000E+00	-7.3567E-03	1.7E-04
6	1	1.996269E+00	-6.42450	0.00000	0.000	-1.371	1.371	0.0000E+00	-2.2410E-02	3.0E-05
9	1	5.128887E+02	-6.17950	0.00000	0.000	-1.284	1.284	0.0000E+00	-6.6778E-01	9.4E-03
10	1	5.132611E+02	-6.07390	0.00000	0.000	-1.409	1.409	0.0000E+00	4.2802E-02	2.7E-02
11	1	5.136277E+02	-5.96829	0.00000	0.000	-1.375	1.375	0.0000E+00	-1.6862E-02	5.9E-02
12	1	5.139777E+02	-5.86269	0.00000	0.000	-1.284	1.284	0.0000E+00	2.1026E-01	2.7E-02
13	1	5.143124E+02	-5.75709	0.00000	0.000	-1.219	1.219	0.0000E+00	1.1823E-01	2.8E-02
14	1	5.146321E+02	-5.65148	0.00000	0.000	-1.173	1.173	0.0000E+00	-4.3222E-02	1.6E-02
15	1	5.149371E+02	-5.54588	0.00000	0.000	-1.148	1.148	0.0000E+00	-4.3309E-01	4.3E-02
16	1	5.152276E+02	-5.44028	0.00000	0.000	-1.052	1.052	0.0000E+00	-3.7151E-02	3.9E-02
17	1	5.155039E+02	-5.33467	0.00000	0.000	-1.013	1.013	0.0000E+00	1.5948E-01	9.7E-04
18	1	5.157663E+02	-5.22907	0.00000	0.000	-0.951	0.951	0.0000E+00	-3.0370E-02	2.7E-02
19	1	5.160152E+02	-5.12347	0.00000	0.000	-0.983	0.983	0.0000E+00	3.9009E-01	8.4E-02
20	1	5.162510E+02	-5.01786	0.00000	0.000	-0.916	0.916	0.0000E+00	1.4082E-01	9.5E-02
21	1	5.164743E+02	-4.91226	0.00000	0.000	-0.795	0.795	0.0000E+00	6.6242E-03	3.6E-03
22	1	5.166855E+02	-4.80666	0.00000	0.000	-0.746	0.746	0.0000E+00	-4.1794E-01	4.8E-02
23	1	5.168853E+02	-4.70105	0.00000	0.000	-0.711	0.711	0.0000E+00	-9.3478E-02	4.4E-02
24	1	5.170743E+02	-4.59545	0.00000	0.000	-0.693	0.693	0.0000E+00	5.8029E-02	6.1E-02
25	1	5.172532E+02	-4.48985	0.00000	0.000	-0.654	0.654	0.0000E+00	2.7897E-01	3.4E-02
26	1	5.174227E+02	-4.38424	0.00000	0.000	-0.617	0.617	0.0000E+00	-1.2669E-01	2.0E-02
27	1	5.175835E+02	-4.27864	0.00000	0.000	-0.564	0.564	0.0000E+00	-1.5108E-01	2.5E-02
28	1	5.177364E+02	-4.17303	0.00000	0.000	-0.558	0.558	0.0000E+00	-1.2753E-01	2.6E-02
29	1	5.178823E+02	-4.06743	0.00000	0.000	-0.532	0.532	0.0000E+00	5.8263E-02	8.0E-02
30	1	5.180219E+02	-3.96183	0.00000	0.000	-0.512	0.512	0.0000E+00	-2.4533E-01	1.7E-02

32	1	5.[illegible]853E+02	-3.75062	0.00000	0.000	-0.477	0.477	0.0000E+00	-1.1105E-01	3.1E-02
33	1	5.184108E+02	-3.64502	0.00000	0.000	-0.487	0.487	0.0000E+00	-1.9067E-01	4.5E-02
34	1	5.185332E+02	-3.53941	0.00000	0.000	-0.417	0.417	0.0000E+00	-3.6268E-01	3.0E-02
35	1	5.186533E+02	-3.43381	0.00000	0.000	-0.423	0.423	0.0000E+00	-1.3556E-01	5.1E-02
36	1	5.187717E+02	-3.32821	0.00000	0.000	-0.454	0.454	0.0000E+00	-2.3712E-01	3.1E-02
37	1	5.188893E+02	-3.22260	0.00000	0.000	-0.424	0.424	0.0000E+00	-2.9197E-01	3.8E-02
38	1	5.190068E+02	-3.11700	0.00000	0.000	-0.430	0.430	0.0000E+00	-2.2385E-01	1.9E-02
39	1	5.191248E+02	-3.01140	0.00000	0.000	-0.446	0.446	0.0000E+00	-1.5597E-01	8.1E-03
40	1	5.192439E+02	-2.90579	0.00000	0.000	-0.435	0.435	0.0000E+00	-4.5147E-01	6.4E-02
41	1	5.193648E+02	-2.80019	0.00000	0.000	-0.471	0.471	0.0000E+00	-3.6292E-01	5.7E-02
42	1	5.194882E+02	-2.69459	0.00000	0.000	-0.471	0.471	0.0000E+00	-2.3582E-01	4.8E-03
43	1	5.196145E+02	-2.58898	0.00000	0.000	-0.475	0.475	0.0000E+00	-1.4561E-01	2.8E-02
44	1	5.197445E+02	-2.48338	0.00000	0.000	-0.496	0.496	0.0000E+00	-2.1520E-01	1.2E-02
45	1	5.198787E+02	-2.37778	0.00000	0.000	-0.541	0.541	0.0000E+00	-2.1761E-01	2.7E-02
46	1	5.200176E+02	-2.27217	0.00000	0.000	-0.545	0.545	0.0000E+00	-1.8248E-01	3.9E-02
47	1	5.201622E+02	-2.16657	0.00000	0.000	-0.581	0.581	0.0000E+00	-2.2186E-01	2.5E-02
48	1	5.203129E+02	-2.06097	0.00000	0.000	-0.568	0.568	0.0000E+00	-3.3926E-01	2.4E-02
49	1	5.204708E+02	-1.95536	0.00000	0.000	-0.595	0.595	0.0000E+00	-3.1291E-01	1.9E-02
50	1	5.206365E+02	-1.84976	0.00000	0.000	-0.646	0.646	0.0000E+00	-2.9233E-01	1.7E-02
51	1	5.208113E+02	-1.74416	0.00000	0.000	-0.666	0.666	0.0000E+00	-3.3835E-01	1.6E-02
52	1	5.209964E+02	-1.63855	0.00000	0.000	-0.726	0.726	0.0000E+00	-3.3962E-01	1.8E-02
53	1	5.211932E+02	-1.53295	0.00000	0.000	-0.770	0.770	0.0000E+00	-3.6097E-01	1.7E-02
54	1	5.214037E+02	-1.42734	0.00000	0.000	-0.817	0.817	0.0000E+00	-4.0708E-01	1.5E-02
55	1	5.216300E+02	-1.32174	0.00000	0.000	-0.878	0.878	0.0000E+00	-4.5189E-01	1.5E-02
56	1	5.218749E+02	-1.21614	0.00000	0.000	-0.954	0.954	0.0000E+00	-4.9584E-01	1.6E-02
57	1	5.221418E+02	-1.11053	0.00000	0.000	-1.045	1.045	0.0000E+00	-5.5014E-01	1.6E-02
58	1	5.224349E+02	-1.00493	0.00000	0.000	-1.151	1.151	0.0000E+00	-6.2468E-01	1.6E-02
59	1	5.227598E+02	-0.89933	0.00000	0.000	-1.281	1.281	0.0000E+00	-7.1936E-01	1.6E-02
60	1	5.231233E+02	-0.79372	0.00000	0.000	-1.440	1.440	0.0000E+00	-8.4204E-01	1.6E-02
61	1	5.235347E+02	-0.68812	0.00000	0.000	-1.639	1.639	0.0000E+00	-1.0051E+00	1.6E-02
62	1	5.240063E+02	-0.58252	0.00000	0.000	-1.890	1.890	0.0000E+00	-1.2266E+00	1.6E-02
63	1	5.245545E+02	-0.47691	0.00000	0.000	-2.213	2.213	0.0000E+00	-1.5288E+00	1.6E-02

64	1	5.[illegible]2023E+02	-0.37131	0.00000	0.000	-2.636	2.636	0.0000E+00	[illegible]	[illegible]
65	1	5.[illegible]59818E+02	-0.26571	0.00000	0.000	-3.214	3.214	0.0000E+00	-2.3991E+00	1.5E-02
66	1	5.269339E+02	-0.16010	0.00000	0.000	-3.763	3.763	0.0000E+00	-2.2009E+00	2.9E-02
67	1	5.280203E+02	-0.05450	0.00000	0.000	-4.444	4.444	0.0000E+00	-2.8157E+00	1.5E-02
70	1	8.569598E+02	-0.02500	0.00000	0.000	-17.827	17.827	0.0000E+00	0.0000E+00	6.2E+00
71	1	8.619267E+02	0.00600	0.00000	0.000	-18.546	18.546	0.0000E+00	2.4482E+04	6.3E+00
72	1	6.709679E+02	0.05470	0.00000	0.000	3055.507	3055.507	0.0000E+00	2.4710E+04	5.1E-01
73	1	1.103849E+02	0.10300	0.00000	0.000	6088.548	6088.548	0.0000E+00	2.4778E+04	6.6E-01
74	1	-8.385994E+02	0.15200	0.00000	0.000	9191.287	9191.287	0.0000E+00	2.4707E+04	4.1E+00
75	1	-3.322364E+03	0.25873	0.00000	0.000	9116.159	9116.159	0.0000E+00	-2.0414E+02	1.6E+00
76	1	-5.790910E+03	0.36545	0.00000	0.000	9087.426	9087.426	0.0000E+00	-1.1726E+02	6.8E-02
77	1	-8.250787E+03	0.47218	0.00000	0.000	9062.306	9062.306	0.0000E+00	-7.1606E+01	9.0E-03
78	1	-1.070527E+04	0.57891	0.00000	0.000	9047.450	9047.450	0.0000E+00	-4.0611E+01	4.9E-03
79	1	-1.315669E+04	0.68564	0.00000	0.000	9039.180	9039.180	0.0000E+00	-2.2166E+01	5.8E-03
80	1	-1.560643E+04	0.79236	0.00000	0.000	9034.742	9034.742	0.0000E+00	-1.1741E+01	7.1E-03
81	1	-1.805528E+04	0.89909	0.00000	0.000	9032.418	9032.418	0.0000E+00	-6.0278E+00	1.1E-02
82	1	-2.050368E+04	1.00582	0.00000	0.000	9031.279	9031.279	0.0000E+00	-2.8945E+00	-2.2E-03
83	1	-2.295186E+04	1.11255	0.00000	0.000	9030.742	9030.742	0.0000E+00	-1.2850E+00	1.0E-02
84	1	-2.539995E+04	1.21927	0.00000	0.000	9030.570	9030.570	0.0000E+00	-2.4322E-01	1.1E-03
85	1	-2.784802E+04	1.32600	0.00000	0.000	9030.568	9030.568	0.0000E+00	2.0157E-01	3.1E-03
86	1	-3.029611E+04	1.43273	0.00000	0.000	9030.705	9030.705	0.0000E+00	5.3504E-01	4.7E-03
87	1	-3.274424E+04	1.53945	0.00000	0.000	9030.907	9030.907	0.0000E+00	8.7128E-01	-3.7E-03
88	1	-3.519245E+04	1.64618	0.00000	0.000	9031.204	9031.204	0.0000E+00	1.2181E+00	1.4E-02
89	1	-3.764074E+04	1.75291	0.00000	0.000	9031.615	9031.615	0.0000E+00	1.7069E+00	7.4E-03
90	1	-4.008918E+04	1.85964	0.00000	0.000	9032.203	9032.203	0.0000E+00	2.5929E+00	4.3E-03
91	1	-4.253780E+04	1.96636	0.00000	0.000	9033.121	9033.121	0.0000E+00	4.3779E+00	4.4E-03
92	1	-4.498678E+04	2.07309	0.00000	0.000	9034.867	9034.867	0.0000E+00	8.4929E+00	1.8E-02
93	1	-4.743643E+04	2.17982	0.00000	0.000	9038.415	9038.415	0.0000E+00	1.8382E+01	3.7E-02
94	1	-4.988751E+04	2.28655	0.00000	0.000	9044.877	9044.877	0.0000E+00	2.8448E+01	-3.6E-02
95	1	-5.234070E+04	2.39327	0.00000	0.000	9049.154	9049.154	0.0000E+00	1.0300E+02	-1.1E+00
96	1	-5.480221E+04	2.50000	0.00000	0.000	8971.032	8971.032	0.0000E+00	-6.9180E+03	-3.9E+00
97	1	-5.685394E+04	2.60000	0.00000	0.000	7215.154	7215.154	0.0000E+00	-6.9027E+03	7.1E-01
98	1	-5.846150E+04	2.70000	0.00000	0.000	5423.229	5423.229	0.0000E+00	-7.1797E+03	1.6E-01

```
PERM.DAT;2

========= THE INPUT FILE CONTAINS THE FOLLOWING :
0
*18 2  *6 0  *9 2.54  *46 2  *85 2.0E-6  *86 6.0E-5  S
3  1.0   1
 0.1000E+4   .001754
 0.2000E+4   .00125
 0.3000E+4   .001010
 0.4000E+4   .0008873
 0.5000E+4   .00082304
 0.6000E+4   .0007886
 0.7000E+4   .00078125
 0.8000E+4   .0007955
 0.9000E+4   .00084033
 0.1000E+5   .00090909
 0.1100E+5   .0010121
 0.1200E+5   .0011467
 0.1300E+5   .0013586
 0.1400E+5   .0017094
 0.1500E+5   .0022727
 0.1600E+5   .003125
 0.1700E+5   .0044444
 0.1800E+5   .006993
 0.1900E+5   .011111
 0.1000E+6    1.0     S
4  1.0   3
 0.2000E+3    0.1000E+0
 0.4000E+3    0.2000E+0
 0.5500E+3    0.3000E+0
 0.1300E+4    0.4000E+0
 0.2000E+4    0.5000E+0
 0.3800E+4    0.7000E+0
 0.6400E+4    0.1000E+1
 0.9000E+4    0.1500E+1
 0.1040E+5    0.2000E+1
 0.1120E+5    0.2500E+1
 0.1200E+5    0.3000E+1
 0.1270E+5    0.4000E+1
 0.1320E+5    0.5000E+1
 0.1360E+5    0.7000E+1
 0.1500E+5     0.200E+2
 0.1600E+5     0.500E+2
 0.1690E+5      0.10E+3
 0.1990E+5      0.40E+3
 0.2080E+5       0.1E+4 S
-1

========= END INPUT FILE (Only 79 columns displayed).
```